with RAVE (*29*). Phases calculated from an initial model traced with O (*22*) were combined with the MIR phase probabilities (*30*) to further improve the electron density maps. The model was refined with XPLOR (*31*). NCS restraints were applied at early stages but then removed. The final *R* factor to 2.1 Å was 17.6% (16,879 reflections) and the R_{free} (*32*) was 25.4% (1867 reflections) for 2929 atoms (residues 8 to 185 in two VHR molecules, one sulfate, one Hepes, and 141 ordered water molecules). The root mean square deviation (rmsd) from ideal bonds and angles was 0.016 Å and 1.7 Å, respectively. The rmsd between the two NCS-related molecules was 1.26 Å for all atoms and 0.82 Å for main chain atoms. The VHR coordinates are available from the Brookhaven Protein Data Bank as entry 1VHR.

16. R. L. Stone and J. E. Dixon, *J. Biol. Chem.* **269**, 31323 (1994).
17. J. A. Stuckey *et al.*, *Nature* **370**, 571 (1994).
18. H. L. Schubert, E. B. Fauman, J. A. Stuckey, J. E. Dixon, M. A. Saper, *Protein Sci.* **4**, 1904 (1995).
19. D. Barford, A. J. Flint, N. K. Tonks, *Science* **263**, 1397 (1994).
20. Z. Jia, D. Barford, A. J. Flint, N. K. Tonks, *ibid.* **268**, 1754 (1995).
21. J. Yuvaniyama *et al.*, data not shown. The peptides modeled were Ala-phosphothreonine-Ala and Ala-phosphotyrosine-Ala.
22. T. A. Jones, J. Y. Zou, S. W. Cowan, M. Kjeldgaard, *Acta Crystallogr.* **A47**, 110 (1991).
23. J. A. Stuckey and M. A. Saper, unpublished data.
24. S. P. Kwak, D. J. Hakes, K. J. Martell, J. E. Dixon, *J. Biol. Chem.* **269**, 3596 (1994).
25. We used the secondary structure of VHR and the secondary structure predicted for CL100 and PAC-1 [B. Rost, C. Sander, R. Schneider, *Comput. Appl. Biosci.* **10**, 53 (1994)] together with the CLUSTALV program [D. G. Higgins, A. J. Bleasby, R. Fuchs, *ibid.* **8**, 189 (1992)] to construct a sequence alignment of the three DSPs. To locate the start of the catalytic domain in CL100, corresponding to the α1 helix in VHR, we scanned upstream terminus of the β1 strand for predicted helices in the CL100 sequence that had the best primary sequence alignment with VHR. The catalytic domains of CL100 and PAC-1 were predicted from the alignment to begin at residues 123 and 130, respectively.
26. A. Messerschmidt and J. W. Pflugrath, *J. Appl. Crystallogr.* **20**, 306 (1987).
27. W. Kabsch, *ibid.* **21**, 916 (1988).
28. W. Furey and S. Swaminathan, *Am. Cryst. Assoc. Meeting Abst.* **18**, 73 (1990).
29. G. J. Kleywegt and T. A. Jones, in *From First Map to Final Model*, S. Bailey, R. Hubbard, D. Waller, Eds. (Engineering and Physical Sciences Research Council, Daresbury, UK, 1994), pp. 59–66.
30. R. J. Read, *Acta Crystallogr.* **A46**, 140 (1990).
31. A. T. Brünger, J. Kuriyan, M. Karplus, *Science* **235**, 458 (1987).
32. A. T. Brünger, *Nature* **355**, 472 (1992).
33. Abbreviations for the amino acid residues are as follows: A, Ala; C, Cys; D, Asp; E, Glu; F, Phe; G, Gly; H, His; I, Ile; K, Lys; L, Leu; M, Met; N, Asn; P, Pro; Q, Gln; R, Arg; S, Ser; T, Thr; V, Val; W, Trp; and Y, Tyr.
34. M. L. Connolly, *J. Appl. Crystallogr.* **16**, 548 (1983).
35. A. Nicholls, K. A. Sharp, B. Honig, *Proteins* **11**, 281 (1991).

36. We thank M. Wishart for help with the CL100 and PAC-1 alignments and C. Yuvaniyama for technical support. Supported by the NIH (grant AI34095 to M.A.S. and grants DK18024 and DK18849 to J.E.D.), a National Research Service award to J.M.D. (GM17789), the University of Michigan Multipurpose Arthritis Center (NIH grant P60-AR20557), and Mitotix Inc. J.Y. is a scholar of the Thai Development and Promotion of Science and Technology Talents Project. M.A.S. is a Pew Scholar in the Biomedical Sciences.

28 November 1995; accepted 8 March 1996

Dimerization of TFIID When Not Bound to DNA

Andrew K. P. Taggart and B. Franklin Pugh*

For unknown reasons, the eukaryotic transcription factor TFIID inefficiently recognizes promoters. Human TFIID was found to form highly specific homodimers that must dissociate before DNA binding. TFIID dimers formed through self-association of the TATA-binding polypeptide (TBP) subunit and could be immunoprecipitated with antibodies to $TAF_{II}250$, the core subunit of TFIID. Chemical cross-linking experiments in HeLa cells revealed the presence of TBP dimers in vivo. These findings suggest that dimerization through TBP is the physiological state of TFIID when not bound to DNA. Thus, the inefficiency of TFIID binding to a promoter may be partly attributable to the competitive effect of dimerization.

Transcription of eukaryotic genes requires the formation of a preinitiation complex containing one of three nuclear RNA polymerases and additional basal factors (*1*). Sequence-specific transcriptional activators function, in part, through direct interactions with basal factors, including polymerase-specific TBP-TAF complexes such as SL1, TFIID, and TFIIIB (*2*). In RNA polymerase II transcription of mRNA genes, the binding of TFIID to the promoter is rate-limiting in complex assembly (*3*). Activators might enhance the recruitment of TFIID to the promoter by targeting TAFs (TBP-associated factors) and TFIIA (*3*); however, the exact mechanism by which TFIID is recruited is not known.

The conserved core DNA-binding domain of TBP homodimerizes at low nanomolar concentrations (*4*). Consequently, TBP dimers must dissociate into monomers before they can bind DNA. These findings are consistent with the reported dimeric crystal structure of TBP dimers (*5*). Because TBP is generally complexed with TAFs, the physiological significance of dimerization is dependent on whether TBP-TAF complexes also dimerize.

To test whether TFIID dimerizes, we subjected a partially purified HeLa TFIID fraction (P.7), which contained approximately 20 to 30 nM TBP, to chemical crosslinking with the use of bis(maleimido)hexane (BMH). In the absence of BMH, the TBP present in the P.7 fraction migrated on an SDS-polyacrylamide gel, with a molecular mass of 44 kD (Fig. 1A). In the presence of BMH, a 90-kD species appeared in the P.7 fraction with a mobility indistinguishable from that of cross-linked recombinant TBP dimers. No other major crosslinker-dependent TBP-containing species was detected, even though the TFIID was <0.1% pure. The predominance of the 90-kD species, among a >1000-fold molar excess of nonspecific nuclear proteins, re-

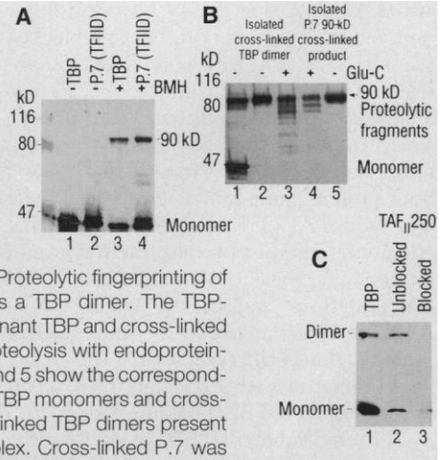

Fig. 1. TBP-TBP cross-linking of TFIID in a crude fraction. (**A**) Crosslinking of the TFIID fraction results in a single TBP-containing 90-kD product. P.7 (TFIID) or purified recombinant TBP were incubated briefly in the absence (−, lanes 1 and 2) or presence (+, lanes 3 and 4) of BMH (*10*). P.7 (TFIID) was generated by passing HeLa nuclear extracts over phosphocellulose and taking a step elution of 0.5 to 0.7 M KCl. Reactions were analyzed by SDS-PAGE and protein immunoblotting with affinity-purified anti-TBP. The purity of the TBP was 99%, and that of the TFIID was <0.1%. (**B**) Proteolytic fingerprinting of the 90-kD band from cross-linked P.7 identifies it as a TBP dimer. The TBP-containing 90-kD products from cross-linked recombinant TBP and cross-linked P.7 (TFIID) were isolated and subjected to limited proteolysis with endoproteinase Glu-C (lanes 3 and 4, respectively) (*11*). Lanes 2 and 5 show the corresponding reaction performed in the absence of proteinase. TBP monomers and cross-linked dimer markers are shown in lane 1. (**C**) Cross-linked TBP dimers present in the P.7 (TFIID) fraction are part of the TFIID complex. Cross-linked P.7 was subjected to immunoprecipitation with anti-TAF_{II}250 in the absence (lane 2, unblocked) or presence (lane 3, blocked) of neutralizing TAF_{II}250 antigen (*12*). The immunoprecipitates were subjected to protein immunoblot analysis with anti-TBP. A TBP dimer marker is shown in lane 1.

Center for Gene Regulation, Department of Biochemistry and Molecular Biology, Pennsylvania State University, University Park, PA 16802, USA.

*To whom correspondence should be addressed. E-mail: bfp2@psuvm.psu.edu

vealed an extraordinary degree of interaction specificity between the two cross-linked proteins and is therefore unlikely to have arisen from random collisions of two noninteracting proteins. The protein cross-linked to TBP could be either another TBP molecule or a different protein with an apparent molecular mass identical to that of TBP.

To determine whether the cross-linked 90-kD species present in the P.7 TFIID fraction represented a TBP dimer, we excised the 90-kD bands that corresponded to the cross-linked recombinant TBP dimers and the cross-linked P.7 TFIID fraction, and we subjected these bands to limited proteolysis with endoproteinase Glu-C. The resulting pattern of bands provided a diagnostic fingerprint of the two cross-linked proteins. The partial proteolytic pattern of the P.7 90-kD species was equivalent to that of pure recombinant cross-linked TBP dimers (Fig. 1B). The similarity of these fingerprints provided strong evidence that the protein cross-linked to TBP was a second molecule of TBP. Had a different protein been cross-linked to TBP, a different proteolytic pattern would have been expected. Thus, the TBP present in the P.7 fraction has the capacity to form dimers in a manner similar to that of recombinant TBP.

We were concerned that the observed P.7 TBP dimers might reflect "free" TBP rather than TBP-TAF complexes. To determine directly whether TFIID dimerizes through TBP-TBP interactions, we used antibodies to $TAF_{II}250$ (anti-$TAF_{II}250$) to immunopurify TFIID from a cross-linked P.7 fraction. $TAF_{II}250$ is the core subunit of TFIID upon which most of the other TAFs and TBP bind (6). $TAF_{II}250$ does not appear to be a component of other previously described TBP-TAF complexes, and thus it represents a marker for TFIID. Cross-linked TBP dimers were immunoprecipitated with anti-$TAF_{II}250$ (Fig. 1C). To control for nonspecific precipitation, we preblocked the anti-$TAF_{II}250$ with pure $TAF_{II}250$ antigen. The preblocked anti-$TAF_{II}250$ was unable to immunoprecipitate TBP dimers, which indicated that TBP was not precipitating nonspecifically. From these data, and from protein immunoblot estimates of the TBP and $TAF_{II}250$ concentrations in P.7 and consideration of total protein content, we conclude that at low nanomolar TFIID concentrations and in the context of a >1000-fold molar excess of other nuclear proteins, the TFIID complex has the capacity to dimerize with extremely high specificity through a TBP-TBP interface.

With recombinant TBP, we envision the dimer interface as encompassing the saddle-shaped DNA-binding domain, as described for the x-ray crystal structure of TBP (5). According to this structure, TBP dimerization is incompatible with DNA binding; recent biochemical studies provide evidence for this interpretation (4). If the same interface applies to TFIID dimers, then TFIID dimerization should also be inhibited by DNA containing a TATA box. As expected, recombinant TBP dimerization was inhibited by TATA but not by an equivalent oligonucleotide containing two point mutations in the TATA box (Fig. 2A). When the P.7 TFIID fraction was incubated with TATA, TBP dimerization was inhibited. Equivalent amounts of the mutant TATA had little effect (Fig. 2A). The pattern of dimerization inhibition was reproducible over a range of nonspecific competitor DNA concentrations. Full inhibition of the P.7 dimer signal with TATA was not observed. The basis for the limited disruption was not investigated but might be the result of a number of factors, including the presence of other TBP-TAF complexes that lack specificity for TATA. Because TATA preferentially inhibits TFIID dimerization relative to an equivalent concentration of mutant TATA, it can be inferred that TFIID dimerization competes with DNA binding.

Under conditions where recombinant TBP predominates as dimers (as measured by gel filtration and protein affinity chromatography), the yield of cross-linked dimers is relatively low (~10%) (4). Inasmuch as the yield of cross-linked TFIID dimers is also in the same range, we surmised that much of the TFIID in the P.7 fraction is present as dimers. We investigated this possibility with gel filtration chromatography. TFIID, as detected by protein immunoblotting with anti-$TAF_{II}250$, eluted primarily in a single peak with an apparent native mass of ~1800 kD (Fig. 2B, nonspecific DNA). However, when TFIID was incubated with TATA, its apparent native mass decreased to ~1000 kD (Fig. 2B, TATA oligonucleotide), which is roughly half of that obtained in the presence of a nonspecific DNA. This size reduction would be expected if TATA is preventing TFIID dimerization. Because the bulk of $TAF_{II}250$ eluted at ~1800 kD (dimer range) and not at ~1000 kD (monomer range), at low concentrations (2 to 5 nM) much of the TFIID in the P.7 fraction appears to be dimeric when not bound to DNA. The observation that TFIID's native size decreased by roughly half upon TATA binding indicates that when not bound to DNA, TFIID is most likely dimerizing with itself (or another large TBP-TAF complex), as opposed to dimerizing with free TBP.

The propensity for TFIID to dimerize at low nanomolar concentrations in vitro suggests that TBP also dimerizes in vivo, where the TBP concentration is >1 μM (7). To test this possibility, we incubated HeLa cells in the presence or absence of crosslinker. The extent of global protein crosslinking was assessed by SDS–polyacrylamide gel

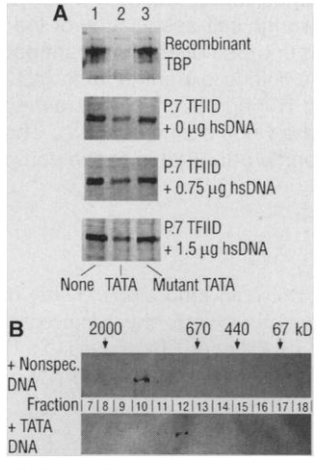

Fig. 2. TATA binding prevents dimerization. **(A)** TATA inhibits crosslinking of TBP. Recombinant TBP (upper panel) or P.7 (TFIID, lower three panels) were incubated in the absence (lane 1) or presence of either a TATA (TATAAAA, lane 2) or a mutant TATA (TAAGAAA, lane 3) oligonucleotide (*13*). Reactions were then treated with BMH, and TBP was detected by protein immunoblotting, as described in Fig. 1. The lower three panels represent cross-linked reactions performed in the presence of increasing amounts of nonspecific herring sperm DNA (hsDNA), as indicated. **(B)** Reduction in the mass of the TFIID complex upon TATA binding. P.7 was incubated in the presence of TATA DNA oligonucleotide or nonspecific control dG-dC DNA (nonspec. DNA) and then subjected to Superose 6 gel filtration (*14*). Results equivalent to the control were obtained in the absence of DNA. Elution of TFIID was monitored by probing protein immunoblots with anti-$TAF_{II}250$. Elution peaks of molecular mass standards are indicated.

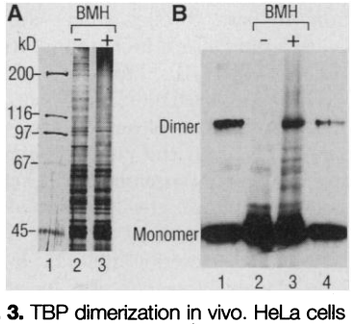

Fig. 3. TBP dimerization in vivo. HeLa cells were either mock- or BMH-treated (*15*). **(A)** Portions of the mock-treated (lane 2) and BMH-treated (lane 3) cells were analyzed for total protein content by SDS-PAGE followed by silver staining. Molecular mass markers are shown in lane 1. **(B)** The mock-treated (lane 2) and BMH-treated (lane 3) cells were extracted with GuHCl, and the TBP was immunopurified and subjected to SDS-PAGE followed by protein immunoblotting. TBP dimer markers are shown in lanes 1 and 4.

electrophoresis (PAGE) followed by silver staining. Some proteins were entirely cross-linked into species of high molecular mass, whereas others showed little change (Fig. 3A). To analyze TBP, we extracted cross-linked and non–cross-linked cells with guanidine hydrochloride (GuHCl) and then immunopurified and analyzed the TBP by protein immunoblotting. When cells were treated with BMH, a 90-kD species appeared that was not present in mock-treated controls (Fig. 3B). The 90-kD species exactly comigrated with recombinant TBP dimers, which suggests that the 90-kD species represents TBP dimers cross-linked in vivo.

In actively growing HeLa cells, a large proportion of TBP is likely to be bound to transcriptionally active promoters, and thus monomeric. Because we cannot assess the efficiency of TBP crosslinking in HeLa cells, only a lower limit of the dimer concentration can be estimated. If we assume that TBP dimers cross-link in vivo with the same efficiency as do TBP dimers in vitro, then a lower limit of ~10% of the TBP is estimated to be dimeric in HeLa cells under standard growth conditions (Fig. 3B). If the efficiency of crosslinking in vivo is lower than that of crosslinking in vitro, then the data lead to a higher estimate of dimers in vivo. The minimal concentration of endogenous TBP dimers is estimated to be in the range of ~100 nM, which is well above the concentration necessary for dimer formation in vitro.

We envision the dimer interface of TFIID as overlapping with the DNA-binding surface in the conserved saddle-shaped domain of TBP (Fig. 4). This arrangement is based on the crystal structure of TBP dimers (*5*). We cannot exclude the possibility that the dimers detected here are different from that observed in the crystal structure. However, our previous biochemical observations that the TBP dimer interface is located in its COOH-terminal domain, is hydrophobic, and is sequestered when bound to TATA as a monomer (*4*) are consistent with the TBP crystal structure. Thus, Fig. 4 represents the most parsimonious interpretation of the data.

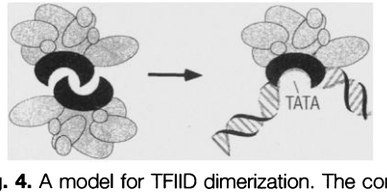

Fig. 4. A model for TFIID dimerization. The concave saddle-shaped DNA-binding domain of TBP (black) is envisioned to encompass the dimerization interface. Dimers must dissociate in order for TFIID monomers to bind DNA. Because we have no direct evidence that TAFs (gray) affect the dimerization process, the cartoon excludes their interactions. However, TAFs may function to modulate the dimerization process.

If TFIID forms dimers that do not bind DNA, then why does TFIID (and possibly other TBP-TAF complexes) dimerize? Dimerization might keep TBP from nonspecifically binding to much of the chromosomal DNA. TBP has a high intrinsic affinity for nonspecific DNA (*8*); once bound, TBP is slow in dissociating and can assemble functional transcription complexes (*8*). Although the high affinity of TBP for nonspecific DNA may have implications with regard to TBP function at TATA-less promoters, it also raises a concern that TBP-TAF complexes would become sequestered in a sea of nonspecific DNA present throughout the genome. However, if TBP-TAF complexes masked the DNA-binding surface of TBP through dimerization, then nonspecific binding would be minimized. Given this possibility, some promoter-bound transcriptional activators might couple dimer-to-monomer conversion of TBP-TAF complexes to promoter-specific DNA binding.

REFERENCES AND NOTES

1. L. Zawel and D. Reinberg, *Annu. Rev. Biochem.* **64**, 533 (1995).
2. R. Tjian and T. Maniatis, *Cell* **77**, 55 (1994).
3. P. M. Lieberman and A. J. Berk, *Genes Dev.* **5**, 2441 (1991); W. Wang, J. D. Gralla, M. Carey, *ibid.* **6**, 1716 (1992); P. M. Lieberman and A. J. Berk, *ibid.* **8**, 995 (1994); N. Klages and M. Strubin, *Nature* **374**, 822 (1995); S. Chatterjee and K. Struhl, *ibid.*, p. 820.
4. R. A. Coleman, A. K. P. Taggart, L. R. Benjamin, B. F. Pugh, *J. Biol. Chem.* **270**, 13842 (1995).
5. D. B. Nikolov *et al.*, *Nature* **360**, 40 (1992); D. B. Nikolov and S. K. Burley, *Nature Struct. Biol.* **1**, 621 (1994).
6. R. O. Weinzierl, B. D. Dynlacht, R. Tjian, *Nature* **362**, 511 (1993).
7. A. K. P. Taggart, A. J. Jackson, B. F. Pugh, data not shown; K. Kato *et al.*, *Nucleic Acids Res.* **22**, 1179 (1994).
8. R. A. Coleman and B. F. Pugh, *J. Biol. Chem.* **270**, 13850 (1995).
9. A. K. P. Taggart, T. S. Fisher, B. F. Pugh, *Cell* **71**, 1015 (1992).
10. Preparation of HeLa P.7 and recombinant TBP has been described (*4, 9*) [B. F. Pugh, in *In Vitro Transcription and Translation Protocols*, M. J. Tymms, Ed. (Humana, Totowa, NJ, 1995), vol. 37, pp. 359–367]. Reactions at 23°C contained 20 mM tris-acetate (pH 7.5), 4 mM $MgCl_2$, 4 mM spermidine, 0.1 mM EDTA, 5% glycerol, 75 mM potassium glutamate, 0.01% nonidet-40, bovine serum albumin (BSA, 5 μg/ml), 9% (v/v) dimethyl sulfoxide, and either 0.1 mg of P.7 and 25 ng of heparin in a volume of 50 μl or 28 ng of recombinant human TBP and 1 μg of polydeoxyguanylic-deoxycytidylic acid [poly(dG-dC)] in a volume of 10 μl. Similar results were obtained when poly(dG-dC), heparin, or BSA were omitted. BMH (Pierce; 0.1 mM for 30 s for TBP, 1 mM for 90 s for P.7) was included where indicated. TBP reactions were quenched by addition of PSB [375 mM tris-Cl (pH 6.8), 3% SDS, 10% glycerol, 5% β-mercaptoethanol, and 0.05% bromphenol blue]. P.7 reactions were quenched with 0.25 M β-mercaptoethanol, and the proteins were precipitated with trichloroacetic acid (TCA) and resuspended in PSB. Samples were subjected to SDS-PAGE on a 7.8% gel, and TBP was visualized by protein immunoblotting (alkaline phosphatase method) with TBP–affinity-purified anti-TBP.
11. Proteolytic fingerprinting was performed on either 1.5 μg of cross-linked recombinant TBP or 3 mg of cross-linked P.7 that had been subjected to SDS-PAGE, transferred to nitrocellulose, and the 90-kD region excised according to F. M. Ausubel *et al.*, Eds., *Current Protocols in Molecular Biology* (Wiley, New York, 1994).
12. Immunoprecipitation of cross-linked P.7 (30 μg) was performed essentially as described (*9*) with 3 μl of $TAF_{II}250$ serum covalently coupled to protein A–sepharose. Blocked antibodies were preincubated with 25 μg of pure $TAF_{II}250$ (248C) antigen. Bound proteins were eluted with PSB and subjected to SDS-PAGE on a 7.8% gel. TBP was detected by protein immunoblotting with biotinylated TBP–affinity-purified anti-TBP. Proteins were visualized with streptavidin–horseradish peroxidase (Pierce) and enhanced chemiluminescence (ECL, Amersham).
13. P.7 (0.1 mg) was cross-linked as described (*10*), except that the heparin was replaced with 2.5 μg of poly(dG-dC) and herring sperm DNA, as indicated. Where indicated, reactions also contained 2 nmol of either TATA (upper strand, 5′-GGAATTCGGGC-TATAAAAGGGGGATCCG-3′) or mutant TATA (upper strand, 5′-GGAATTCGGGCTAAGAAAGGGG-GATCCG-3′) double-stranded oligonucleotides, and were incubated at 30°C for 1 hour before adding BMH.
14. P.7 (0.13 mg) was incubated with either 0.3 nmol of dG-dC DNA (upper panel) or 0.3 nmol of TATA oligonucleotide (lower panel) in a volume of 250 μl for 45 min at 30°C, as described (*10*). Reactions were then injected onto a Superose 6 (Pharmacia) gel filtration column equilibrated with 20 mM tris-acetate (pH 8), 5% glycerol, 2 mM $MgCl_2$, 0.1 mM EDTA, 1 mM dithiothreitol (DTT), 0.1% nonidet-40, and 200 mM potassium glutamate. Fractions (1 ml) were collected and the proteins were precipitated with TCA. Proteins were subjected to SDS-PAGE on a 5% gel and analyzed by protein immunoblotting with affinity-purified anti-$TAF_{II}250$.
15. HeLa cells (4×10^7) were concentrated into 0.5 ml of growth medium by centrifugation and incubated on ice for 30 min. BMH (1 mM) was added to half of the cells; the other half were mock-treated. The cells remained intact during treatment with BMH, as visualized by light microscopy. The cells were incubated at 37°C for 1 hour, then pelleted by centrifugation. Samples (5×10^4 cells) were removed, resuspended in PSB, and subjected to SDS-PAGE on a 7.8% gel. Proteins were stained with silver. The remainder of the cells were resuspended in 1.5 ml of phosphate-buffered saline (PBS) containing 3 mM β-mercaptoethanol, which served to quench any residual BMH. Cells were pelleted again and resuspended in 0.2 ml of PBS. After addition of 4.3 volumes of 8 M GuHCl containing 2 mM DTT, the mixture was homogenized through a 22-gauge needle and heated at 100°C for 5 min. Samples were diluted in HO buffer [20 mM Hepes (pH 7.5), 10% glycerol, 0.1 mM EDTA, 2 mM $MgCl_2$, 0.1 mM DTT, and 0.2 mM phenylmethylsulfonyl fluoride] to a final GuHCl concentration of 1 M. Precipitates were removed by centrifugation at 30,000*g* for 30 min at 4°C, and supernatants were precleared by passage over columns containing 0.2 ml of nonspecific serum covalently cross-linked to 0.2 ml of protein A–sepharose (Pharmacia) [E. Harlow and D. Lane, *Antibodies, a Laboratory Manual*, Cold Spring Harbor Laboratory Press, Cold Spring Harbor, NY, 1988]. Column flow-throughs were incubated with 0.03 ml of anti-TBP serum covalently cross-linked to 0.03 ml of protein A–sepharose overnight at 4°C with constant mixing. The resin was pelleted by centrifugation and washed twice with ~300 bed volumes of HO buffer containing 1 M GuHCl and 0.005% nonidet-40, followed by a wash with HO buffer lacking GuHCl. Bound proteins were eluted with PSB and subjected to SDS-PAGE on a 7.8% gel. TBP was detected by protein immunoblotting (ECL method).

16. Supported by grants from NIH (GM47855) and the Searle Scholars Program/Chicago Community Trust. We thank R. A. Coleman for his efforts on the initial phase of the project and for Fig. 2B, and A. Jackson-Fisher for help with tissue culturing. We are especially grateful to R. Tjian for his encouragement.

5 December 1995; accepted 21 March 1996